

Microtubule Polarity Predicts Direction of Egg Chamber Rotation in *Drosophila*

Ivana Viktorinová^{1,2} and Christian Dahmann^{1,2,*}

¹Institute of Genetics, Technische Universität Dresden, 01062 Dresden, Germany

²Max Planck Institute of Molecular Cell Biology and Genetics, Pfotenhauerstrasse 108, 01307 Dresden, Germany

Summary

Whole-tissue rotations have recently been recognized as a widespread morphogenetic process important for tissue elongation [1–4]. In *Drosophila* ovaries, elongation of the egg chamber involves a global rotation of the follicle epithelium along the anterior-posterior axis [5]. Individual egg chambers rotate either in a clockwise or counterclockwise direction; however, how the symmetry of egg chambers is broken to allow rotation remains unknown. Here we show that at the basal side of follicle cells, microtubules are preferentially aligned perpendicular to the anterior-posterior axis of the egg chamber. Microtubule depolymerization stalls egg chamber rotation and egg chamber elongation. The preferential alignment of microtubules and egg chamber rotation depend on the atypical cadherin Fat2 and the planar polarized Fat2 localization depends on intact microtubules. Moreover, by tracking microtubule plus-end growth in vivo using EB1::GFP, we find that microtubules are highly polarized in the plane of the follicle epithelium. Polarization of microtubules precedes the onset of egg chamber rotation and predicts the direction of rotation. Our data suggest a feedback amplification mechanism between Fat2 localization and microtubule polarity involved in breaking symmetry and directing egg chamber rotation.

Results and Discussion

Microtubules Are Preferentially Aligned Perpendicular to the Long Axis of Egg Chambers

Asymmetries in microtubule organization have emerged as an important principle in specifying axes and establishing polarities within embryos, tissues, and cells [6–10]. To test whether microtubules play a role in establishing the directionality of egg chamber rotation in the *Drosophila* ovary, we first analyzed the spatiotemporal organization of microtubules and compared it to the organization of actin filaments, which were previously shown to be preferentially oriented perpendicular to the anterior-posterior (AP) axis of the egg chamber [11]. Egg chambers of different developmental stages were stained for acetylated Tubulin and F-actin and the basal side of follicle cells was imaged. The orientation of microtubules and F-actin was quantified using the plugin “Directionality” within the software package Fiji [12] (see [Experimental Procedures](#)). During stage 4, the orientation of microtubules and F-actin was moderately, and during stages 5–8 more strongly, biased toward an orientation perpendicular to the AP axis of the egg chamber ([Figures 1A, 1B, 1E, 1F, 1K, 1L, 1O, and 1P](#) and

[Figures S1A–S1J](#) available online). Microtubules tended to be aligned both within cells and between neighboring cells ([Figure 1F](#)), similar to the alignment of actin filaments ([Figure 1E](#)) [11]. During stages 9 and 10a, F-actin continued to be preferentially oriented perpendicular to the AP axis, whereas microtubules were no longer strongly biased in their orientation ([Figures 1I, 1J, 1S, and 1T](#) and [Figures S1K–S1N](#)). In stage 10b, neither microtubules nor actin filaments showed a strong bias in their orientations ([Figures S1O and S1P](#)). We conclude that microtubules are transiently preferentially oriented perpendicular to the AP axis and that the developmental timing of this preferential orientation differs from that of actin filaments.

Microtubule Orientation Requires Fat2

Atypical cadherins play key roles in the establishment of planar polarity in diverse tissues by mediating cell-to-cell interactions [13]. In the follicle epithelium, planar polarity depends on the atypical cadherin Fat2. Fat2 is required for the preferential orientation of F-actin and the elongation of the egg chamber [14]. To test whether the preferential orientation of microtubules also depends on Fat2, we analyzed the orientation of microtubules in *fat2^{58D}* mutant egg chambers. Microtubules were still aligned within each cell of *fat2^{58D}* mutant egg chambers ([Figures S1Q–S1T](#)); however, microtubules were no longer preferentially oriented perpendicular to the AP axis of the follicle epithelium ([Figures 1C, 1D, 1G, 1H, 1M, 1N, 1Q, and 1R](#)). Depolymerization of F-actin using latrunculin A did not alter the orientation of microtubules ([Figures S1U–S1Y](#)). Thus, the preferential orientation of microtubules relative to the tissue axes requires Fat2 but not intact actin filaments.

Microtubules and Actomyosin Contractility Are Required for Egg Chamber Rotation

Microtubules are important for egg chamber elongation, since adult wild-type flies fed with the microtubule-polymerization-inhibiting drug colchicine produced mainly rounded eggs (85%, $n = 46$ stage 7 egg chambers; [Figures S2A and S2B](#)). Elongation of egg chambers involves the rotation of egg chambers relative to the underlying extracellular matrix [5]. We first characterized the velocity of rotation at different developmental stages. Egg chambers were cultured in vitro and time-lapse movies were obtained. Expression of a functional GFP-tagged form of DE-cadherin, DE-cad::GFP [15], was used to follow cell junctions during egg chamber rotation. At stage 4, egg chambers did not noticeably rotate ([Figures 2A and 2I](#)). During stage 5, egg chambers rotated slowly ($0.17 \pm 0.021 \mu\text{m}/\text{min}$) ([Figures 2B and 2I](#)), and from stage 6 to 8, egg chamber rotation was fastest ($0.46 \pm 0.041 \mu\text{m}/\text{min}$) ([Figures 2C and 2I](#); [Movie S1](#)), consistent with previous results [5]. At mid and late stage 9, no egg chamber rotation was observed ([Figures 2D and 2I](#)). We note that the cessation of egg chamber rotation coincides with the loss of the preferential orientation of microtubules.

To test whether microtubules are required for egg chamber rotation, we fed flies with colchicine and observed egg chambers by time-lapse imaging. In contrast to controls,

*Correspondence: christian.dahmann@mailbox.tu-dresden.de

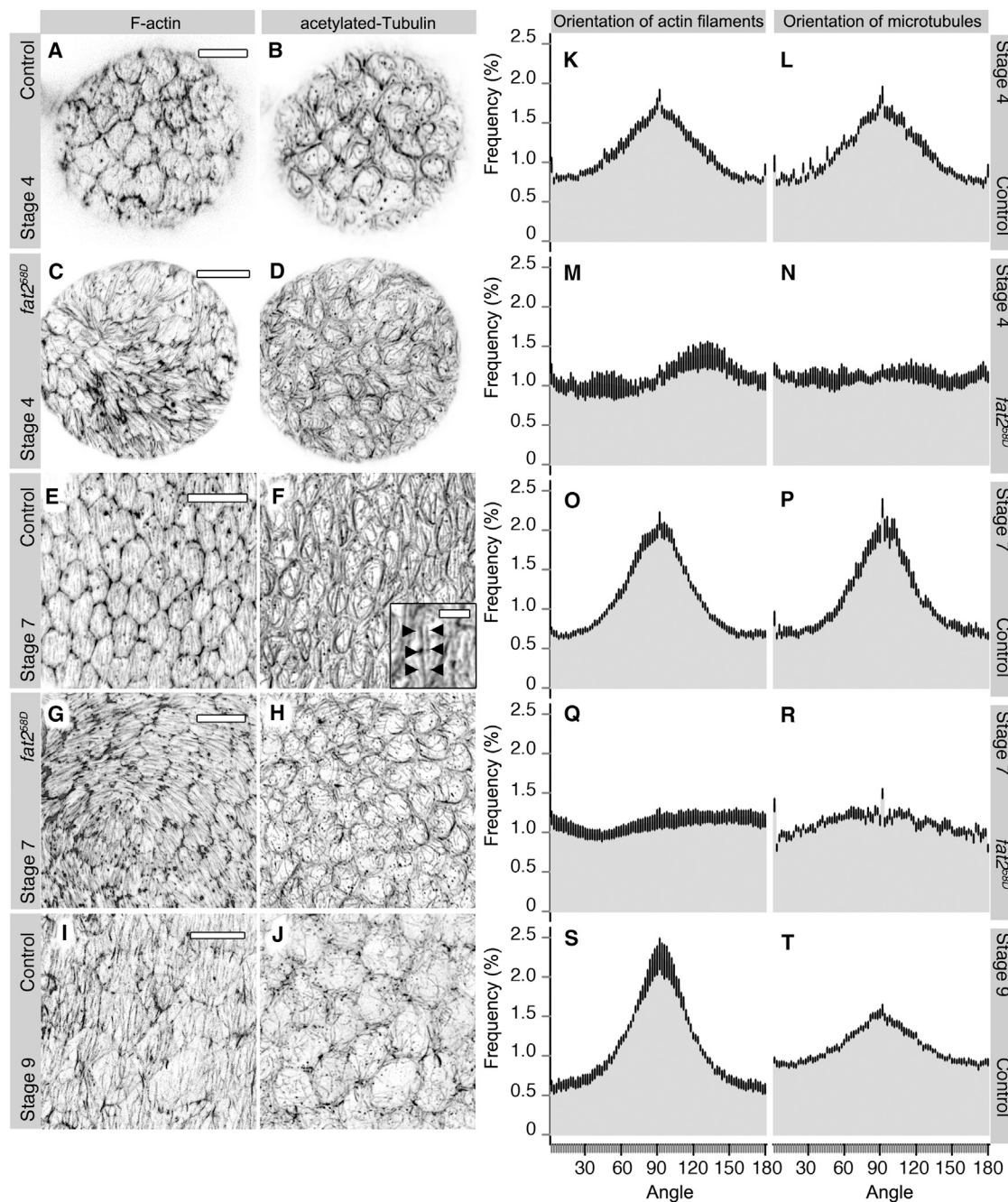


Figure 1. Planar-Polarized Orientation of Microtubules and Actin Filaments

(A–J) Follicle cells of control (A, B, E, F, I, and J) and *fat2^{58D}* mutant (C, D, G, and H) egg chambers of the indicated stages stained for F-actin (A, C, E, G, and I) and acetylated Tubulin (B, D, F, H, and J). Inset in (F) shows higher-magnification view of aligned microtubules (arrowheads). Deconvoluted images of basal views of egg chambers are shown. In these, and all subsequent images, anterior is to the left. Scale bars represent 10 μm (inset represents 2.5 μm). (K–T) Frequency of actin filaments (K, M, O, Q, and S) and microtubules (L, N, P, R, and T) oriented within a 2° interval relative to the AP axis of egg chambers of the indicated stages; 0°/180° denote actin filaments or microtubules parallel to the AP axis. Mean and SEM are shown ($n \geq 10$ egg chambers per stage).

egg chambers of colchicine-fed flies did not rotate (Figure S2C). To test the consequences of acutely inhibiting microtubule polymerization, we added colchicine to ex vivo cultivated egg chambers. Two hours after addition of colchicine, acetylated Tubulin staining was greatly reduced in follicle cells (Figures S2D and S2E). Egg chamber rotation was slowed down approximately 2-fold compared to controls (Figure 2J). Three to four hours after colchicine addition,

the speed of egg chamber rotation was reduced approximately 10-fold to $0.03 \pm 0.011 \mu\text{m}/\text{min}$ (Figures 2E and 2J). Colchicine-treated egg chambers did not show increased cell death and integrity of the follicle epithelium appeared to be mainly intact (Figures S2F–S2I'). We noted, however, that after 4 hr of colchicine treatment, the actin cytoskeleton of cells was perturbed (Figures S2J–S2K'). Preventing actin polymerization by addition of latrunculin A also did not result

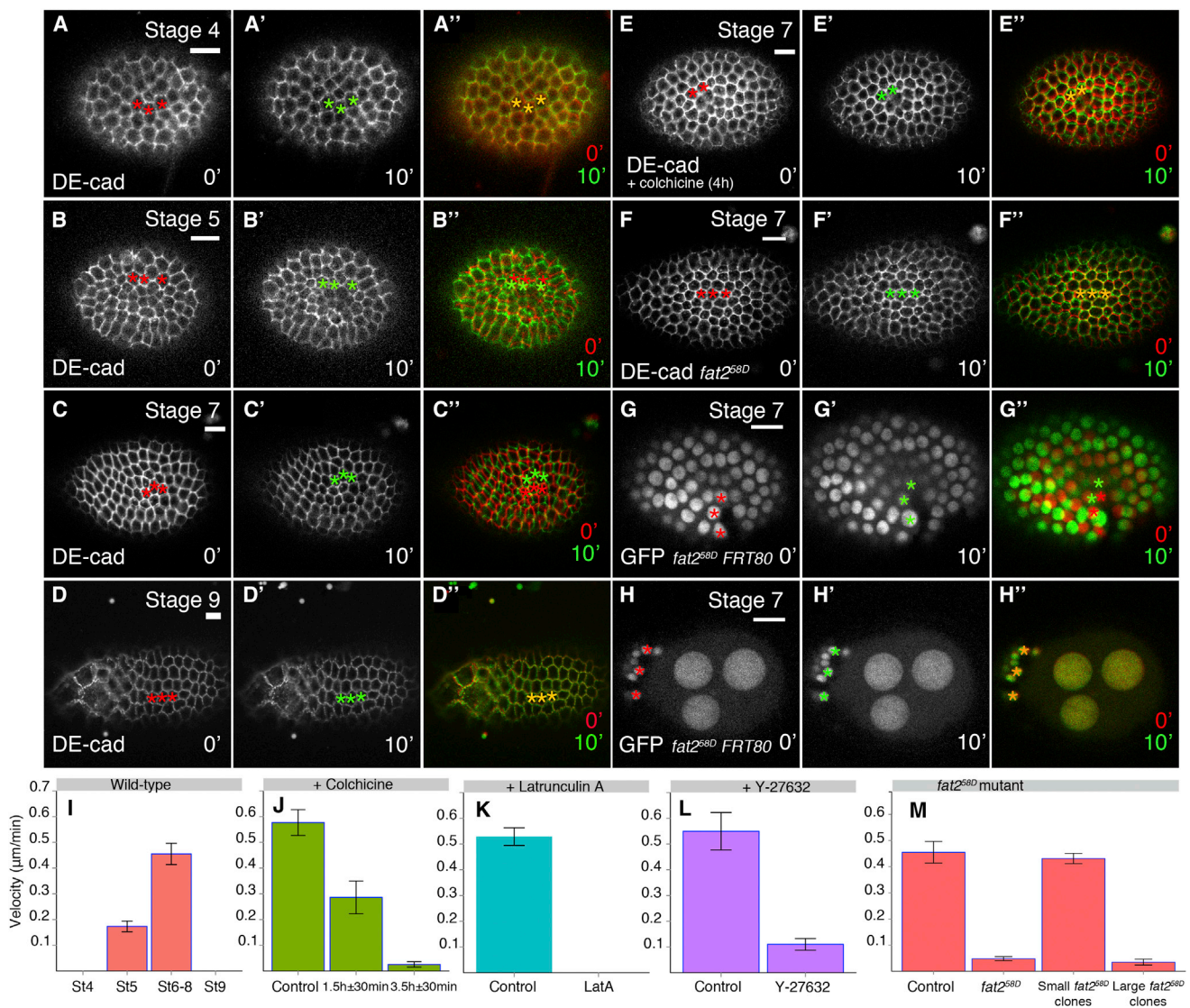


Figure 2. Microtubules, Actomyosin Contractility, and Fat2 Are Required for Egg Chamber Rotation

(A–F'') Time-lapse analysis (0' and 10') of *DE-cad::GFP* ex vivo cultured egg chambers of indicated stages. In (E), colchicine was added for 4 hr prior to imaging. In (F), a *fat2^{58D}* mutant egg chamber is shown. (G–H'') Time-lapse analysis (0' and 10') of egg chambers carrying small (G) and large (H) clones of *fat2^{58D}* mutant follicle cells marked by the absence of nuclear GFP. In (A)–(H''), red and green asterisks mark identical cells at the two time points. The column on the right shows overlays of the 0' and 10' time points. Scale bar represents 10 μm. (I–M) Velocity of egg chamber rotation for untreated egg chambers at the indicated stages (I) and stages 6–8 egg chambers treated for the indicated times with colchicine (J) or 10' min with latrunculin A (K) or 1.5 hr ± 30 min with Y-27632 (L). In (M), the velocity of egg chamber rotation for the indicated genotypes is detailed. Mean and SEM are shown (n ≥ 10 egg chambers per treatment or genotype).

in large-scale cell death (Figures S2L and S2M) but rapidly inhibited egg chamber rotation. Ten minutes after addition of latrunculin A to cultivated egg chambers, rotation was essentially stopped (Figure 2K). Likewise, addition of the Rho-kinase inhibitor Y-27632 [16], which inhibits nonmuscle Myosin II activity, to cultivated egg chambers resulted in a greatly reduced speed of egg chamber rotation and no large-scale cell death (Figure 2L; Figure S2N). Thus, egg chamber rotation relies on actomyosin-based force generation, as is generally observed during collective cell migration [17]. Microtubules might only be indirectly required for egg chamber rotation by influencing the organization of the actin cytoskeleton or by transporting molecules that are required for rotation.

Fat2 Is Required for Egg Chamber Rotation

Egg chamber rotation depends on interactions between the follicle cells and extracellular matrix components [5]. To test whether cell-to-cell interactions are also important, we analyzed the role of Fat2 in egg chamber rotation. To this end, we used live imaging to analyze cultured control and *fat2^{58D}* mutant stage 7 egg chambers. Control egg chambers rotated with an average velocity of 0.46 ± 0.041 μm/min (Figure 2M), consistent with previous results [5]. In contrast, the average velocity of *fat2^{58D}* mutant egg chambers was reduced about 10-fold to 0.05 ± 0.007 μm/min (Figures 2F and 2M; Movie S2). Thus, Fat2 and therefore cell-to-cell interactions play an important role during egg chamber rotation.

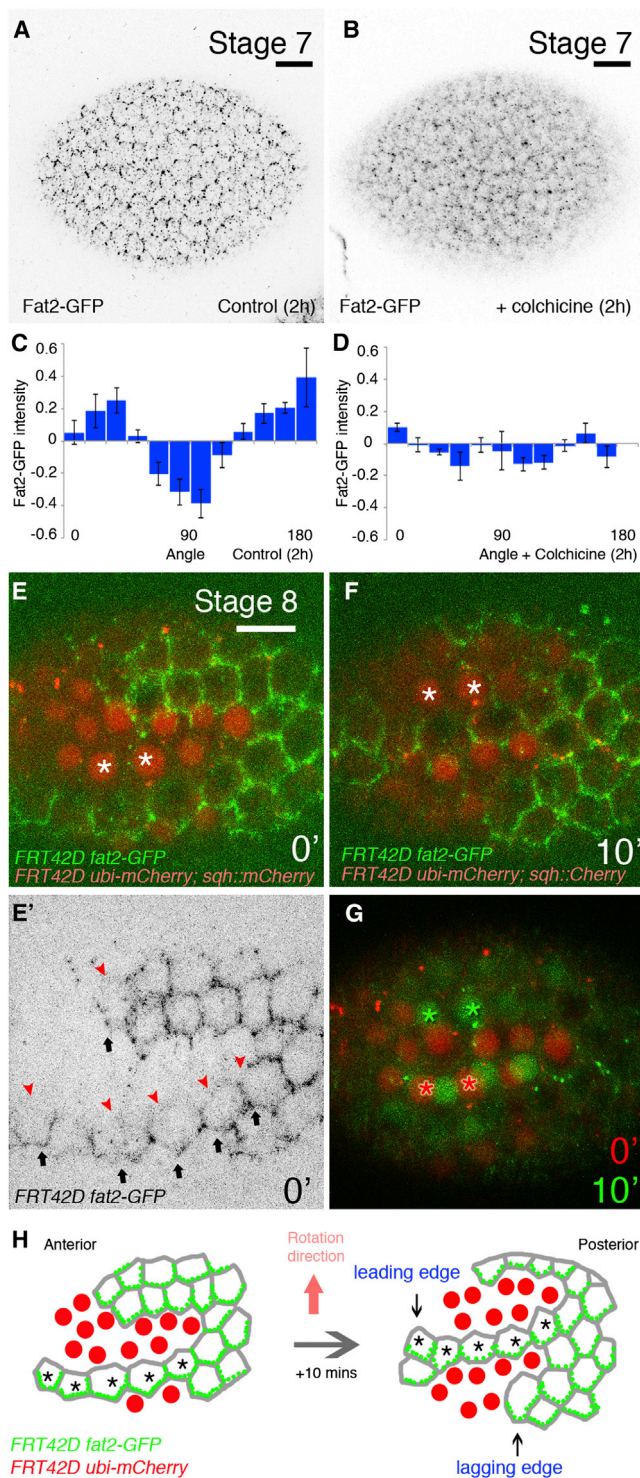


Figure 3. Fat2-GFP Is Located on the Lagging Edge of Follicle Cells

(A–D) Basal views of control (A and C) and colchicine-treated (B and D) stage 7 egg chambers expressing Fat2-GFP. (C and D) The relative Fat2-GFP pixel intensities for cell membranes oriented in 15° intervals; 0°/180° denote cell membranes parallel to the AP axis of the egg chamber. Mean and SEM are shown. Control: n = 556 cell membranes in three egg chambers. Colchicine-treated: n = 524 cell membranes in three egg chambers. (E–G) Time-lapse analysis (0' and 10') of ex vivo cultured stage 8 egg chambers expressing Fat2-GFP (green) in clones of cells marked by the absence of mCherry (red). Basal cell outlines are visualized by sqh::mCherry (see also Figures S3B and S3C). At the clone border, Fat2-GFP localizes to the cell edges

We have previously shown that egg chamber shape and the planar orientation of actin filaments depend on the ratio of wild-type to *fat2* mutant cells within the follicle epithelium [14, 18]. To test whether the ratio of wild-type to *fat2*^{58D} mutant cells within the follicle epithelium is also important for egg chamber rotation, we generated small- and large-sized *fat2*^{58D} clones and analyzed the rotation of cultivated stage 7 egg chambers. The velocity of rotation of egg chambers displaying few small clones of *fat2*^{58D} mutant cells was similar to the velocity of control egg chambers (Figures 2G and 2M). In contrast, egg chambers in which the majority of follicle cells was mutant for *fat2*^{58D}, the velocity was approximately reduced 10-fold (Figures 2H and 2M), similar to the velocity of nonmosaic *fat2*^{58D} egg chambers. Thus, egg chamber rotation depends on the orchestrated activity of follicle cells, perhaps by propagating a cue that coordinates the migratory activities of cells within the follicle epithelium.

Fat2-GFP Localizes to the Lagging Edge of Follicle Cells in a Microtubule-Dependent Manner

The asymmetric distribution of proteins is fundamental to the establishment of planar polarity [19–23]. Fat2 localizes during stages 4 and 5 to cellular vertices ([14]; Figure S3A) and during later stages is enriched in a coherent zigzag pattern on cell junctions oriented nearly parallel to the AP axis of egg chambers [14]. At these later stages, Fat2 localizes only to one and the same side of cells throughout the follicle epithelium [14]. This chiral planar distribution of Fat2 does not require intact actin filaments (Figures S3D and S3E) but depends on the presence of microtubules, since colchicine treatment of cultivated egg chambers resulted in a nearly uniform distribution of Fat2 along the cell edges (Figures 3A–3D). To test whether the chiral planar distribution of Fat2 correlates with the direction of egg chamber rotation, we generated clones of follicle cells expressing Fat2-GFP and monitored the direction of egg chamber rotation by live imaging. Fat2-GFP was consistently (28 out of 28 analyzed egg chambers) enriched on cell junctions facing the lagging edge of follicle cells (Figures 3E–3H). These data demonstrate an asymmetric Fat2 protein distribution in migrating follicle cells.

Microtubules Grow Preferentially Opposite to the Direction of Egg Chamber Rotation

We next tested whether the growth of microtubules in follicle cells is polarized. To this end, we followed the movement of a GFP-tagged microtubule plus-end binding protein, EB1::GFP [10], at the basal side of follicle cells by live imaging at different developmental stages. EB1::GFP showed a comet-like signal with bright fronts and darker tails (Figure S4A; Movie S3), as reported in other cells [24, 25]. EB1::GFP moved along straight tracks within follicle cells (Figures S4B and S4C) with an average speed during stages 4–9 of $0.230 \pm 0.019 \mu\text{m/s}$, similar to other studies ($0.235 \pm 0.048 \mu\text{m/s}$ [24]; $0.27 \pm 0.054 \mu\text{m/s}$ [10]). To test whether the movement of EB1::GFP has a preferential orientation, we tracked the movement of more than 1,000 individual EB1::GFP comets per stage and determined the orientation of EB1::GFP tracks relative to the AP axis of the egg chambers. During stages 4–8, the vast

facing to the bottom in the image (arrows) and is absent from cell edges facing to the top (arrowheads). (G) Overlay of the mCherry channels of images in (E) and (F) show the direction of egg chamber rotation. Asterisks mark identical cells at the two time points. Scale bar represents 10 μm . (H) Schematic representation of the images is shown in (E)–(G).

Microtubules and Egg Chamber Rotation

5

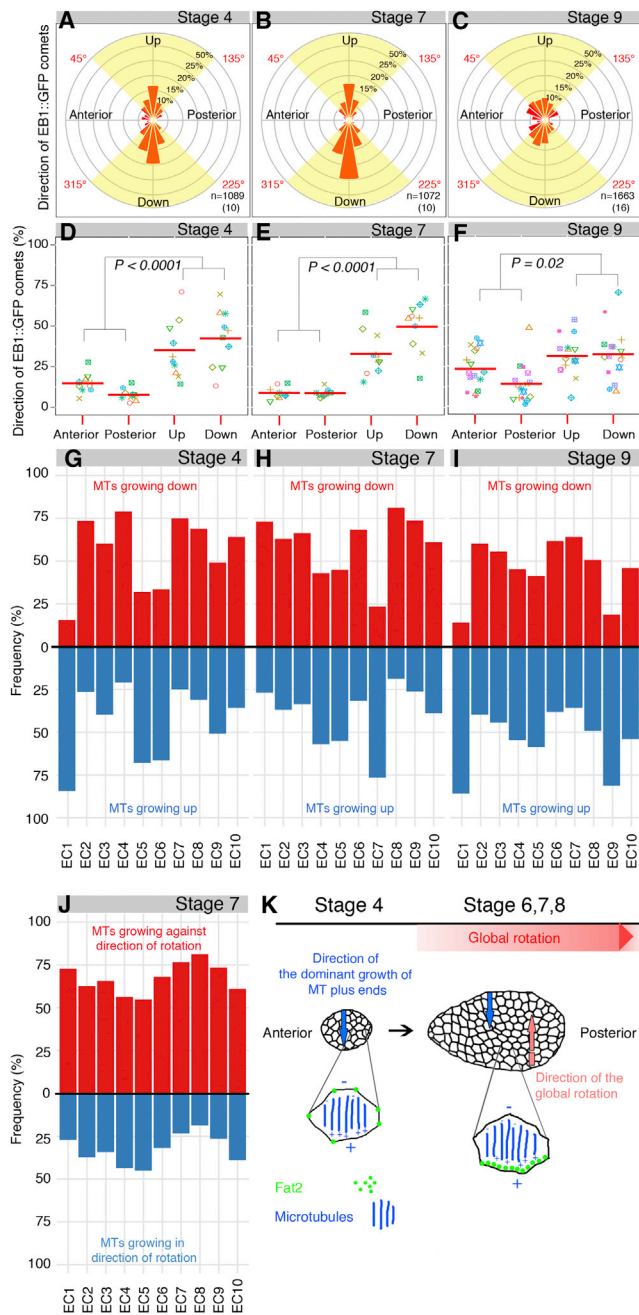


Figure 4. Direction of Microtubule Plus-End Growth Predicts Direction of Egg Chamber Rotation

(A–C) Angular distributions of the direction of EB1::GFP comets at the basal side of follicle cells in egg chambers of the indicated stages for 20° bins. The numbers on the circles give the fraction of EB1::GFP comets in a bin as a percentage of the total number of comets analyzed; 0° corresponds to comets shooting toward anterior. The numbers of comets and egg chambers analyzed at each stage are indicated at the lower right. (D–F) Fractions of EB1::GFP comets shooting toward anterior (>315°–45°), posterior (>135°–225°), up (>45°–135°), or down (>225°–315°) within an image frame for individual egg chambers (indicated by the different colors and shapes) of the indicated stages. Mean and p values are shown. (G–I) Frequency of microtubule plus ends growing down or up within an image frame for ten individual egg chambers (ECs) of the indicated stages. (J) Frequency of microtubule plus ends growing against or in the direction of rotation for ten individual stage 7 ECs. In (G)–(J), only EB1::GFP comets shooting toward up quadrants or down quadrants were analyzed. (K) Summary and model. At stage 4, microtubules grow with their plus ends preferentially either

majority of EB1::GFP comets moved along tracks that were nearly perpendicular to the AP axis of egg chambers (Figures 4A, 4B, 4D, and 4E and Figures S4D–S4G), consistent with the preferential orientation of microtubules during these developmental stages (see Figure 1). By contrast, during stage 9, when microtubule orientation is no longer biased (see Figure 1), the movements of EB1::GFP comets no longer showed a strong preferential direction (Figures 4C and 4F).

We next tested whether the movement of EB1::GFP comets has a preferential direction (chirality) in individual egg chambers during stages 4 to 9. To this end, we analyzed the frequency of EB1::GFP comets moving up or down in image frames of ten individual egg chambers for each stage. Only two out of ten egg chambers observed at stage 9 showed obvious preferences for EB1::GFP comets moving either up or down (Figure 4I); however, such a preference was highly pronounced during stages 6 to 8 (Figure 4H and Figures S4H and S4I). Thus, microtubule plus-end growth is transiently chiral planar polarized.

To test whether the chirality of microtubule plus-end growth is correlated with the orientation of egg chamber rotation during stages 5 to 8, we analyzed the movement of EB1::GFP by high-speed time-lapse imaging (2 s intervals for a total of 3–4 min) followed by long-term recording (30 s intervals for a total of 10–20 min) to analyze the rotation of egg chambers. The preferential direction of EB1::GFP movement was strictly anticorrelated with the direction of rotation of individual egg chambers during stages 5–8 (Figure 4J; Figures S4H and S4I; n ≥ 10 egg chambers per stage). We conclude that the growth of microtubules is polarized in a way that in a given egg chamber, microtubules grow within follicle cells preferentially in a unique direction (clockwise or counterclockwise) around the AP axis. The direction of microtubule plus-end growth predicts the direction of egg chamber rotation.

Egg chamber rotation is only initiated during stage 5 (see Figure 2I; [5]). To test whether the chiral planar growth of microtubule plus ends is initiated concomitant with or prior to the onset of egg chamber rotation, we analyzed the movement of EB1::GFP comets in stage 4 egg chambers. EB1::GFP comets moved preferentially in the same direction within individual egg chambers (Figure 4G), demonstrating that the planar chirality of microtubule plus-end growth precedes the onset of egg chamber rotation.

Conclusions

We have identified the planar polarity of microtubule plus ends as early visible manifestation of breaking chiral symmetry in the *Drosophila* follicle epithelium. Microtubule plus-end polarity precedes egg chamber rotation and predicts the direction of egg chamber rotation (Figure 4K). Egg chamber rotation relies on actomyosin-based force generation and the coordination of migratory activity of cells within the follicle epithelium by Fat2. Fat2 localizes in a microtubule-dependent fashion to the lagging edge of follicle cells, the edge of a cell toward which microtubule plus ends predominantly grow. We cannot, however, currently distinguish whether the polarized localization of Fat2 depends only on the planar-polarized microtubules or also on some other population of microtubules in

clockwise or counterclockwise within individual egg chambers. Egg chambers do not rotate. Fat2 localizes to cell corners. During stages 6–8, egg chambers rotate, microtubule plus ends grow against the direction of rotation, and Fat2 has redistributed to the lagging edge of cells.

the cell. Nevertheless, it will be interesting to investigate in the future whether the planar-polarized distribution of Fat2 is mediated by microtubule plus-end-directed vesicular transport, as has been previously shown for Frizzled in the developing *Drosophila* wing [10]. Fat2 is in turn required for the planar orientation of microtubules in the follicle epithelium. Our data are consistent with a model in which a weak planar polarity of microtubules is established early during egg chamber development. A feedback amplification mechanism between Fat2 localization and microtubule polarity later on refines microtubule polarity to establish robust chiral planar polarity in the tissue, which in turn directs egg chamber rotation. This work demonstrates that establishing the chirality of egg chamber rotation is intricately intertwined with the mechanisms that establish planar polarity in the follicle epithelium.

Supplemental Information

Supplemental Information includes four figures, Supplemental Experimental Procedures, and three movies and can be found with this article online at <http://dx.doi.org/10.1016/j.cub.2013.06.014>.

Acknowledgments

We are grateful to J.-Y. Tinevez and D.J. White for developing the plugin “Directionality,” to I. Henry for his introduction to R, and to M. Osterfield for advice on live imaging. We thank S. Eaton, H. Ohkura, and T. Uemura for fly stocks, the Developmental Studies Hybridoma Bank for antibodies, and S. Eaton, H. Gutzeit, and P. Tomancak for critical comments on the manuscript. This work was supported by grants from the Human Frontier Science Program (RGP0052/2009 to C.D.) and the Deutsche Forschungsgemeinschaft (DA586/10 and DA586/14 to C.D.).

Received: January 10, 2013

Revised: May 8, 2013

Accepted: June 5, 2013

Published: July 3, 2013

References

- Bastock, R., and St Johnston, D. (2011). Oogenesis: matrix revolutions. *Curr. Biol.* **21**, R231–R233.
- Bilder, D., and Haigo, S.L. (2012). Expanding the morphogenetic repertoire: perspectives from the *Drosophila* egg. *Dev. Cell* **22**, 12–23.
- Gates, J. (2012). *Drosophila* egg chamber elongation: insights into how tissues and organs are shaped. *Fly (Austin)* **6**, 213–227.
- He, L., Wang, X., and Montell, D.J. (2011). Shining light on *Drosophila* oogenesis: live imaging of egg development. *Curr. Opin. Genet. Dev.* **21**, 612–619.
- Haigo, S.L., and Bilder, D. (2011). Global tissue revolutions in a morphogenetic movement controlling elongation. *Science* **331**, 1071–1074.
- Li, R., and Gunderson, G.G. (2008). Beyond polymer polarity: how the cytoskeleton builds a polarized cell. *Nat. Rev. Mol. Cell Biol.* **9**, 860–873.
- Vladar, E.K., Bayly, R.D., Sangoram, A.M., Scott, M.P., and Axelrod, J.D. (2012). Microtubules enable the planar cell polarity of airway cilia. *Curr. Biol.* **22**, 2203–2212.
- Marcinkevicius, E., and Zallen, J.A. (2013). Regulation of cytoskeletal organization and junctional remodeling by the atypical cadherin Fat. *Development* **140**, 433–443.
- Harumoto, T., Ito, M., Shimada, Y., Kobayashi, T.J., Ueda, H.R., Lu, B., and Uemura, T. (2010). Atypical cadherins Dachsous and Fat control dynamics of noncentrosomal microtubules in planar cell polarity. *Dev. Cell* **19**, 389–401.
- Shimada, Y., Yonemura, S., Ohkura, H., Strutt, D., and Uemura, T. (2006). Polarized transport of Frizzled along the planar microtubule arrays in *Drosophila* wing epithelium. *Dev. Cell* **10**, 209–222.
- Gutzeit, H.O. (1990). The microfilament pattern in the somatic follicle cells of mid-vitellogenic ovarian follicles of *Drosophila*. *Eur. J. Cell Biol.* **53**, 349–356.
- Schindelin, J., Arganda-Carreras, I., Frise, E., Kaynig, V., Longair, M., Pietzsch, T., Preibisch, S., Rueden, C., Saalfeld, S., Schmid, B., et al. (2012). Fiji: an open-source platform for biological-image analysis. *Nat. Methods* **9**, 676–682.
- Thomas, C., and Strutt, D. (2012). The roles of the cadherins Fat and Dachsous in planar polarity specification in *Drosophila*. *Dev. Dyn.* **241**, 27–39.
- Viktorinová, I., König, T., Schlichting, K., and Dahmann, C. (2009). The cadherin Fat2 is required for planar cell polarity in the *Drosophila* ovary. *Development* **136**, 4123–4132.
- Huang, J., Zhou, W., Dong, W., Watson, A.M., and Hong, Y. (2009). From the Cover: Directed efficient, and versatile modifications of the *Drosophila* genome by genomic engineering. *Proc. Natl. Acad. Sci. USA* **106**, 8284–8289.
- Uehata, M., Ishizaki, T., Satoh, H., Ono, T., Kawahara, T., Morishita, T., Tamakawa, H., Yamagami, K., Inui, J., Maekawa, M., and Narumiya, S. (1997). Calcium sensitization of smooth muscle mediated by a Rho-associated protein kinase in hypertension. *Nature* **389**, 990–994.
- Iliina, O., and Friedl, P. (2009). Mechanisms of collective cell migration at a glance. *J. Cell Sci.* **122**, 3203–3208.
- Viktorinová, I., Pismen, L.M., Aigouy, B., and Dahmann, C. (2011). Modelling planar polarity of epithelia: the role of signal relay in collective cell polarization. *J. R. Soc. Interface* **8**, 1059–1063.
- Bayly, R., and Axelrod, J.D. (2011). Pointing in the right direction: new developments in the field of planar cell polarity. *Nat. Rev. Genet.* **12**, 385–391.
- Goodrich, L.V., and Strutt, D. (2011). Principles of planar polarity in animal development. *Development* **138**, 1877–1892.
- McNeill, H. (2010). Planar cell polarity: keeping hairs straight is not so simple. *Cold Spring Harb. Perspect. Biol.* **2**, a003376.
- Singh, J., and Mlodzik, M. (2012). Planar Cell Polarity Signaling: Coordination of cellular orientation across tissues. *Wiley Interdiscip. Rev. Dev. Biol.* **1**, 479–499.
- Vichas, A., and Zallen, J.A. (2011). Translating cell polarity into tissue elongation. *Semin. Cell Dev. Biol.* **22**, 858–864.
- Mimori-Kiyosue, Y., Shiina, N., and Tsukita, S. (2000). The dynamic behavior of the APC-binding protein EB1 on the distal ends of microtubules. *Curr. Biol.* **10**, 865–868.
- Rogers, S.L., Wiedemann, U., Häcker, U., Turck, C., and Vale, R.D. (2004). *Drosophila* RhoGEF2 associates with microtubule plus ends in an EB1-dependent manner. *Curr. Biol.* **14**, 1827–1833.